

Immunohistochemical detection of ROS1 is useful for identifying *ROS1* rearrangements in lung cancers

Akihiko Yoshida¹, Koji Tsuta¹, Susumu Wakai¹, Yasuhito Arai², Hisao Asamura³, Tatsuhiro Shibata², Koh Furuta¹, Takashi Kohno⁴ and Ryoji Kushima¹

¹Division of Pathology and Clinical Laboratories, National Cancer Center Hospital, Tokyo, Japan; ²Division of Cancer Genomics, Center for Medical Genomics, National Cancer Center Research Institute, Tokyo, Japan; ³Division of Thoracic Surgery, National Cancer Center Hospital, Tokyo, Japan and ⁴Division of Genome Biology, National Cancer Center Research Institute, Tokyo, Japan

The recent discovery and characterization of an oncogenic *ROS1* gene fusion in a subset of lung cancers has raised significant clinical interest because small molecule inhibitors may be effective to these tumors. As lung cancers with *ROS1* rearrangements comprise only 1–3% of lung adenocarcinomas, patients with such tumors must be identified to gain optimal benefit from molecular therapy. Recently, immunohistochemical analyses using a novel anti-*ROS1* rabbit monoclonal antibody (D4D6) have shown promise for accurate identification of *ROS1*-rearranged cancers. To validate this finding, we compared the immunostaining results of tissue microarrays (TMAs) containing 17 *ROS1*-rearranged and 253 *ROS1*-non-rearranged lung carcinomas. All 17 *ROS1*-rearranged cancers showed *ROS1* immunoreactivity mostly in a diffuse and moderate-to-strong manner with an H-score range of 5–300 (median, 260). In contrast, 69% of *ROS1*-non-rearranged cancers lacked detectable immunoreactivity, whereas the remaining 31% showed reactivity mainly in a weak or focal manner. The H-score for the entire *ROS1*-non-rearranged group ranged from 0 to 240 (median, 0). The difference in H-score between the two cohorts was statistically significant, and the H-score cutoff (≥ 150) allowed optimal discrimination (94% sensitivity and 98% specificity). Similar but slightly less-specific performance was achieved using the extent of diffuse ($\geq 75\%$) staining or $\geq 2+$ staining intensity as cutoffs. *CD74-ROS1* and *EZR-ROS1* fusions were significantly associated with at least focal globular immunoreactivity and plasma membranous accentuation, respectively, and these patterns were specific to *ROS1*-rearranged cases. Although full-length *ROS1* is expressed in some *ROS1*-non-rearranged cases, we showed that establishment of an optimal set of interpretative criteria makes *ROS1* immunohistochemistry a valuable method to rapidly and accurately screen lung cancer patients for appropriate molecular therapy.

Modern Pathology (2014) 27, 711–720; doi:10.1038/modpathol.2013.192; published online 1 November 2013

Keywords: adenocarcinoma; immunohistochemistry; lung; *ROS1*

A significant proportion of lung carcinomas are not amenable to surgical management because they present at advanced stages or recur after primary resection.¹ Molecular subclassification of tumors is particularly important for such cases because genetic change is the major determinant of the effectiveness of targeted molecular therapy. For example, lung cancers with anaplastic lymphoma kinase (*ALK*)

gene rearrangements are susceptible to treatment with *ALK* inhibitors (for example, crizotinib),² and those with a mutation in the gene encoding epidermal growth factor receptor (*EGFR*) respond to *EGFR* inhibitors (for example, erlotinib and gefitinib).³ The recent discovery and characterization of oncogenic *ROS1* gene fusion in lung adenocarcinomas^{4–8} have expanded the list of the molecular subsets of lung cancers. *ROS1* encodes a protein tyrosine kinase that belongs to the insulin receptor family. *ROS1* is fused to one of a number of genes in lung cancers, including *CD74*, *SLC34A2*, *EZR*, *LRIG3*, *SDC4*, *TPM3*, *FIG* (also known as *GOPC*), *CCDC6*, and *KDEL2*.^{4–7,9–12} In these fusions, the 3' region of *ROS1* encoding its kinase

Correspondence: Dr A Yoshida, MD, PhD, Department of Pathology and Clinical Laboratories, National Cancer Center Hospital, 5-1-1 Tsukiji, Chuo-ku, Tokyo 104-0045, Japan.
E-mail: akyoshid@ncc.go.jp
Received 5 July 2013; accepted 2 September 2013; published online 1 November 2013

domain is fused to the 5' region of the respective partner gene. The fusion encodes a chimeric protein with constitutive kinase activity that initiates oncogenic intracellular signal transduction cascades.^{7,13} Preclinical data suggest that *ROS1*-rearranged cancers respond to ALK inhibitors,^{5,6,9} and a recent clinical trial¹⁴ revealed a marked inhibition of this molecular subclass by crizotinib. These data underscore the clinical importance of identifying *ROS1*-rearranged cancers to customize treatment.

As *ROS1*-rearranged lung cancer comprises only 1–3% of lung adenocarcinomas,^{4–9,15} the appropriate patients must be selected who will benefit most from molecular therapy. Although these cancers are diagnosed using the reverse transcriptase-polymerase chain reaction (RT-PCR) and/or fluorescence *in situ* hybridization (FISH), molecular assays are time-consuming, costly, and not suitable for rapid screening. Unfortunately, clinicopathologic features serve poorly for this purpose. Although *ROS1*-rearranged cancer tends to occur in young non-smokers,^{5,7,8} clinical parameters are not sufficiently predictive for successful triage. Similarly, although the characteristic histological features have been described for this subset,^{7,8} their role is likely limited in the care of patients who present at advanced stages where molecular therapy is most needed because such features are present in only a subset of fusion-positive cases typically as a focal manner.⁸ Recently, Rimkunas *et al*⁹ developed a novel anti-ROS1 rabbit monoclonal antibody (D4D6) and proposed the utility of immunohistochemistry for identifying *ROS1*-rearranged cancers by showing its 100% (8/8) sensitivity and 100% (138/138) specificity when compared with break-apart FISH. However, the issue is still controversial because other investigators^{16,17} observed *ROS1* expression in a significant proportion (20–30%) of lung carcinomas likely unassociated with gene rearrangement. In this study, we applied this D4D6 antibody to a large number of lung cancers with a known *ROS1* rearrangement status to test the utility of immunohistochemistry for molecular subtyping.

Materials and methods

Case Selection

After receiving approval from the institutional review board at the National Cancer Center in Tokyo, we constructed TMAs containing 346 primary lung adenocarcinomas by using a tissue-arraying instrument (Azumaya, Tokyo, Japan). The tumors were collected from surgical resections with curative intent performed at the National Cancer Center Hospital from 1997 to 2009, and they were enriched for *EGFR* wild-type cases by using high-resolution melting analysis¹⁸ (27% were *EGFR* mutants). Each tumor was sampled by collecting

2.0-mm-diameter cores from two different representative sites. The TMAs were analyzed by using *ROS1* break-apart FISH as described below. After exclusion of 84 cases that either failed to hybridize or lacked an adequate amount of evaluable tumor tissue in the cores, 9 *ROS1*-rearranged cases and 253 *ROS1*-non-rearranged cases were identified. The ranges of rearrangement-positive cell rate in the *ROS1*-rearranged and *ROS1*-non-rearranged cohorts were 42–84% and 0–8%, respectively; no case showed borderline 10–20% range of rearrangement signals. To expand the rearrangement-positive cohort, eight *ROS1*-rearranged tumors (seven adenocarcinomas and one adenosquamous carcinoma) that were separately identified using RT-PCR were also included, and they were similarly assembled in a TMA as duplicate 2.0-mm cores, except for one case with a limited amount of tissue. Of the 17 *ROS1*-rearranged cancers included in this study, 15 were previously reported with their detailed clinicopathologic findings.⁸

FISH

FISH assays were performed using a custom *ROS1* break-apart probe set (Chromosome Science Labo Inc., Sapporo, Japan), which hybridizes with the neighboring 5' telomeric (RP11-48A22, labeled with SpectrumGreen) and 3' centromeric (RP11-1036C2, labeled with SpectrumOrange) sequence of the *ROS1* gene. This probe set is designed to detect all known *ROS1* fusions, including *FIG-ROS1*, which is unlikely to be detected using a previously described design^{5,8} in which the 5' probe hybridizes with the RP11-835I21 region. The present probe was internally validated to identify the *FIG-ROS1* fusion in the U-118MG glioblastoma cell line.¹⁹ FISH images were captured using the Metafer Slide Scanning Platform (MetaSystems, Altussheim, Germany) to facilitate analysis. Fifty non-overlapping tumor cells with at least one each of 5' and 3' signals were examined for each case. The rearrangement-positive cells were defined as those with split signals or isolated red (3') signals. The specimen was considered as *ROS1*-rearranged if the rearrangement-positive cells constituted $\geq 15\%$ of the enumerated tumor cells. This 15% cutoff value was previously established to accurately differentiate between *ROS1*-rearranged and *ROS1*-non-rearranged cases based on RT-PCR data.⁸

Multiplex RT-PCR

Multiplex RT-PCR was performed as described previously⁸ and was designed to detect the fusion transcripts as follows: *CD74-ROS1*, *EZR-ROS1*, *SLC34A2-ROS1*, *FIG-ROS1*, *LRIG3-ROS1*, *SDC4-ROS1*, and *TPM3-ROS1*. The PCR products were subjected to Sanger sequencing.

ROS1 Immunohistochemistry

Immunohistochemical staining was performed on TMA sections, except for one *ROS1*-rearranged case that was evaluated using the whole section. Four-micrometer-thick sections were deparaffinized, and heat-induced epitope retrieval was performed with targeted retrieval solution (pH 9) (Dako, Carpinteria, CA, USA). The slides were treated with 3% hydrogen peroxide for 20 min to block endogenous peroxidase activity. The slides were then incubated with a primary antibody against ROS1 (D4D6, 1:100, Cell Signaling Technology, Danvers, MA, USA) at 4 °C overnight. Reactivity was detected using the EnVision-FLEX+ (Dako). Immunostained slides were scored using the H-score method, which is based on the percentages of cells stained with intensities of 0, 1+, 2+, and 3+ as follows: $H\text{-score} = \sum [\text{intensity} (0, 1, 2, 3) \times \text{extent of each staining intensity} (\%)]$. H-scores range from 0 to 300. Intensity 0 was defined as no detectable staining. Intensity 1+ was defined as reactivity only detectable at high magnification ($\times 20$ – 40 objective). More intense reactivity was divided into moderate (2+) and strong (3+) based on the ease of detection at low magnification ($\times 4$ objective).

Statistical Analysis

All data were analyzed using SPSS version 20.0 (IBM Corporation, Somers, NY, USA). The Fisher's exact test and the Mann–Whitney *U*-test were used for categorical and continuous data, respectively. *P*-values were two-tailed, and *P* < 0.05 was considered significant.

Results

Immunohistochemical Analysis of ROS1 Expression

Immunostaining was evaluated based on the results of two TMA cores for each tumor, except for 12 *ROS1*-non-rearranged cases for which scoring was performed on one core that contained tumor tissue. All 17 *ROS1*-rearranged cancers showed ROS1 immunoreactivity primarily in a diffuse and moderate-to-strong manner with an H-score range of 5–300 (median, 260, Figure 1a). In contrast, most (69%) *ROS1*-non-rearranged cancers lacked detectable immunoreactivity (Figure 1b), whereas the remaining 31% showed some degree of reactivity, mostly in a weak or focal manner (Figure 1c). The H-score for the entire *ROS1*-non-rearranged group ranged from 0 to 240 (median, 0). The difference in H-score between the two cohorts was statistically significant (*P* < 0.001). The staining pattern in all the 95 immunopositive cases (17 *ROS1*-rearranged and 78 *ROS1*-non-rearranged cases) was cytoplasmic. The background lung parenchyma included in the TMA cores occasionally showed ROS1 staining in macro-

phages (14 cases) and in reactive type II pneumocytes (15 cases, Figure 1d).

Establishment of Immunostaining Interpretative Criteria to Predict Gene Rearrangement

The distribution of H-scores is illustrated in Figure 2. As the scores were continuous rather than sharply separated into two categories, we attempted to establish an optimal set of criteria that helps to predict *ROS1* rearrangement. As there is no universally accepted H-score as a cutoff in the literature, we set a range of H-scores (0, 5, 10, 20, 50, 100, 150, 200, and 250) as the cutoff and calculated test sensitivity and specificity for each condition. This analysis showed that an H-score of ≥ 150 best discriminated between *ROS1*-rearranged and -non-rearranged cases with 94% sensitivity and 98% specificity (Table 1). Moreover, we set an array of more conventional criteria based on staining extent or intensity and similarly calculated test sensitivity and specificity for each condition. The best separation was achieved when immunopositivity was defined as $\geq 75\%$ tumor cells labeling with any intensity, and it produced 94% sensitivity and 90% specificity (Table 1). Similar results (94% sensitivity and 87% specificity) were obtained when the immunopositivity was defined as $\geq 2+$ intensity in any extent.

Correlation of ROS1 Fusion Partner With Staining Pattern

Among 17 rearrangement-positive cases, data on *ROS1* fusion partners were available for 15 cases as follows: *CD74-ROS1* (C6;R34), *n* = 10; *EZR-ROS1* (E10;R34), *n* = 4; *SLC34A2-ROS1* (S13del2046;R34), *n* = 1. Among 10 *CD74-ROS1*-positive tumors, six showed at least focal globular immunoreactivity, comprising 1–6 round to ovoid intense intracytoplasmic signals measuring 3–8 μm in diameter. These globules appeared randomly distributed within the cytoplasm rather than restricted to the perinuclear zones. They occurred within the background of weaker cytoplasmic staining and were occasionally associated with adjacent fine granularity. This pattern was observed in almost all cells in one case (Figure 3a), whereas it was observed in a subset of cells in the remaining five cases (Figure 3b). This pattern was not observed in the remaining four *CD74-ROS1*-positive tumors and five *ROS1*-rearranged tumors with partners other than *CD74*. The association between a globular pattern and *CD74* as a fusion partner was statistically significant (*P* = 0.044). One tumor (P16) that was not subjected to RT-PCR also showed this globular pattern.

Among the four *EZR-ROS1*-positive tumors, three showed at least focal plasma membranous linear accentuation with occasional fine granular quality.

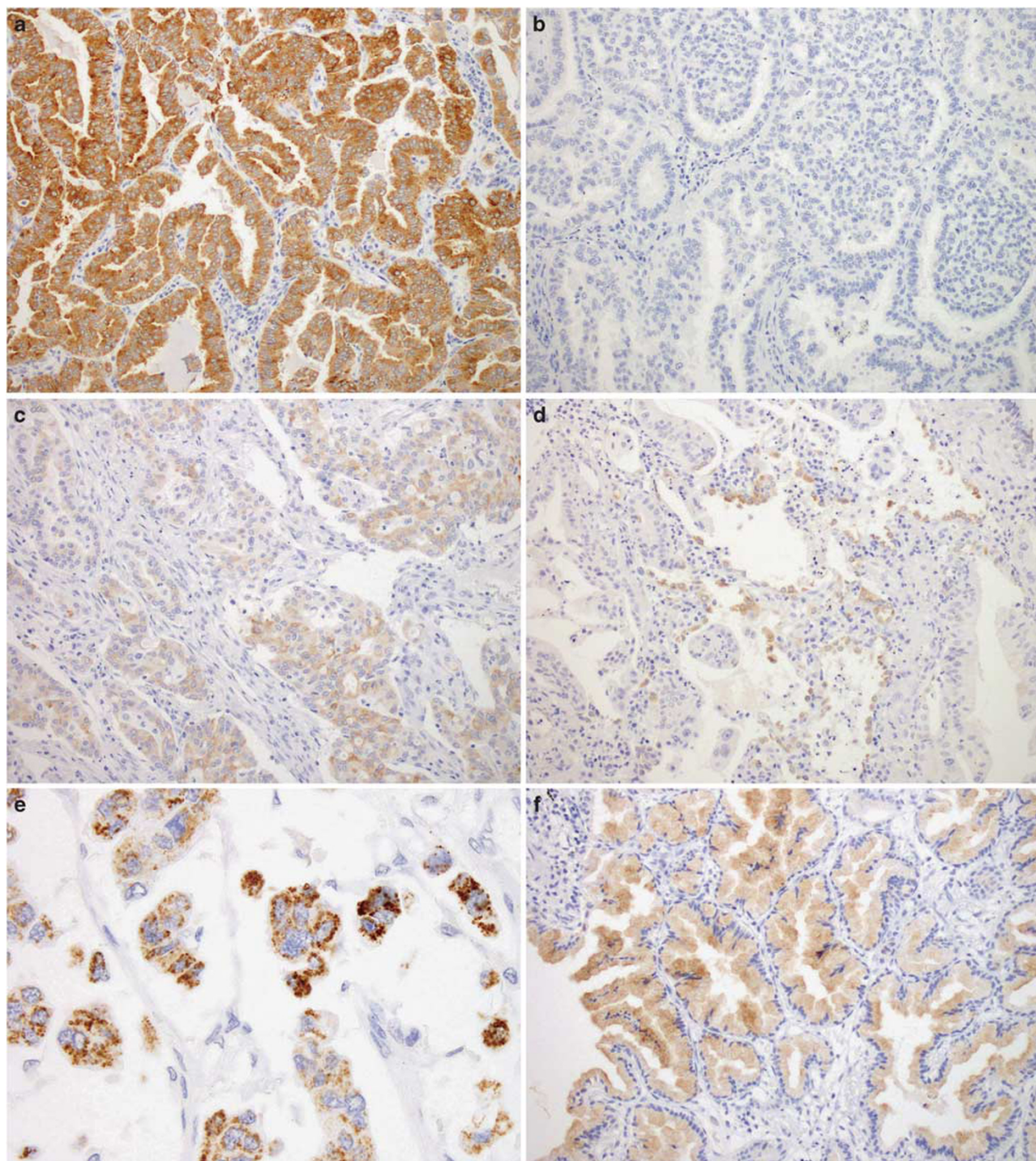


Figure 1 Most *ROS1*-rearranged cancers showed diffuse and moderate-to-strong *ROS1* immunoreactivity (a), whereas 69% of *ROS1*-non-rearranged cancers lacked detectable *ROS1* expression (b). The remaining 31% of *ROS1*-non-rearranged cancers expressed *ROS1*, mainly in a weak or focal manner (c). Adjacent lung parenchyma showed occasional *ROS1* expression in reactive type II pneumocytes (d). The pattern of *ROS1* reactivity in some *ROS1*-non-rearranged tumors was distinctly granular (e). The majority of invasive mucinous adenocarcinomas showed *ROS1* reactivity despite the lack of a gene rearrangement (f).

Membranous accentuation appeared on the lateral surface of tumor cells in two cases (Figure 3c) and along the apical surface in one case (Figure 3d). This pattern was not observed in the remaining *EZR-ROS1*-positive tumor and 11 *ROS1*-rearranged tu-

mors with partners other than *EZR*. The association between membranous accentuation and *EZR* as a fusion partner was statistically significant ($P=0.009$). None of the 78 rearrangement-negative tumors with *ROS1* expression showed globular

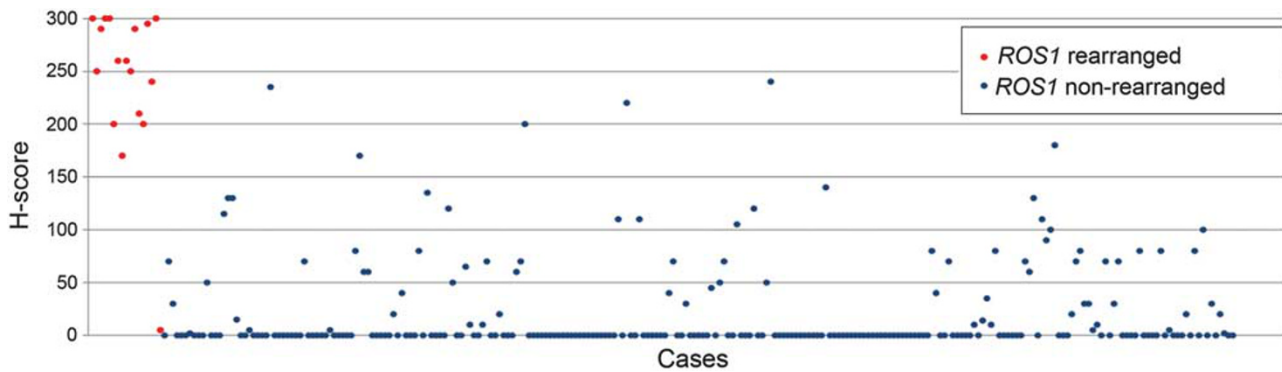


Figure 2 Distribution of H-scores for lung adenocarcinomas determined by using ROS1 immunohistochemistry. Red dots represent scores of ROS1-rearranged cases, and blue dots represent scores of ROS1-non-rearranged cases.

Table 1 Performance of ROS1 immunohistochemical analysis to predict ROS1 rearrangement using an array of interpretative criteria

Criteria	The number of ROS1-rearranged cases that meet the criteria (total N = 17)	The number of ROS1-non-rearranged cases that meet the criteria (total N = 253)	Sensitivity	Specificity
H-score				
H-score > 0	17	78	100%	69%
H-score ≥ 5	17	76	100%	70%
H-score ≥ 10	16	72	94%	72%
H-score ≥ 20	16	65	94%	74%
H-score ≥ 50	16	49	94%	81%
H-score ≥ 100	16	20	94%	92%
H-score ≥ 150 ^a	16	6	94%	98%
H-score ≥ 200	15	4	88%	98%
H-score ≥ 250	12	0	71%	100%
Extent				
Extent ≥ 1%	17	78	100%	69%
Extent ≥ 5%	17	76	100%	70%
Extent ≥ 10%	16	70	94%	72%
Extent ≥ 50%	16	48	94%	81%
Extent ≥ 75% ^a	16	25	94%	90%
Extent = 100%	15	6	88%	98%
Intensity				
Intensity ≥ 2 + ^a	16	33	94%	87%
Intensity = 3 +	13	8	76%	97%

^aIndicates optimal criteria to predict ROS1 rearrangement.

reactivity or plasma membranous accentuation. The only *SLC34A2-ROS1*-positive case showed solid cytoplasmic ROS1 staining without distinctive features.

Analysis of Immunopositive ROS1-Non-Rearranged Cases

Among the 78 immunopositive ROS1-non-rearranged cases, 16 (21%) showed at least focal granular-staining

quality (Figure 1e), and the remaining 62 cases (79%) showed non-granular solid staining. Twelve tumors (15%) were morphologically classified as invasive mucinous adenocarcinoma (formerly mucinous bronchioloalveolar carcinoma with invasion;²⁰ Figure 1f). They comprised 80% of the 15 invasive mucinous adenocarcinomas included here. Among the remaining 238 non-mucinous ROS1-non-rearranged cases, we did not observe a clear correlation between histology and immunoreactivity.

Analysis of ROS1-Rearranged Cases with Low Immunostaining

Two ROS1-rearranged tumors exhibited less ROS1 staining than did the other 15 cases. One (P8) was an adenocarcinoma that was almost purely composed of signet-ring cells (Figure 4a) whose ROS1 rearrangement (*EZR-ROS*) was confirmed using FISH and RT-PCR. The tumor showed diffuse but weak to moderate ROS1 reactivity with an H-score of 170 (Figure 4b). The other outlier case (P17) was an adenocarcinoma resected from a non-smoking Japanese woman in her 50's. It was positive for FISH with 78% of tumor cells having rearrangement patterns mostly in the form of isolated 3' signals (Figure 5a). FISH positivity was confirmed by examining multiple microscopic fields and by using a probe set of different design (RP11-1036C2 for the 3' probe and RP11-835I21 for the 5' probe). However, this case showed only weak focal staining with an H-score of 5 (Figure 5b), and this modest reactivity was confirmed using the whole section. Interestingly, multiplex RT-PCR using fresh frozen material did not detect an ROS1 fusion transcript. Further, this case harbored a deletion of *EGFR* exon 19 and showed diffuse strong immunoreactivity, detected by using an EGFR deletion (E746-A750del)-specific antibody (clone 6B6, 1:100, Cell Signaling Technology) (Figure 5c). As the disease was in the early stage, the patient was successfully treated by surgical resection and did not undergo molecular-targeted therapy.

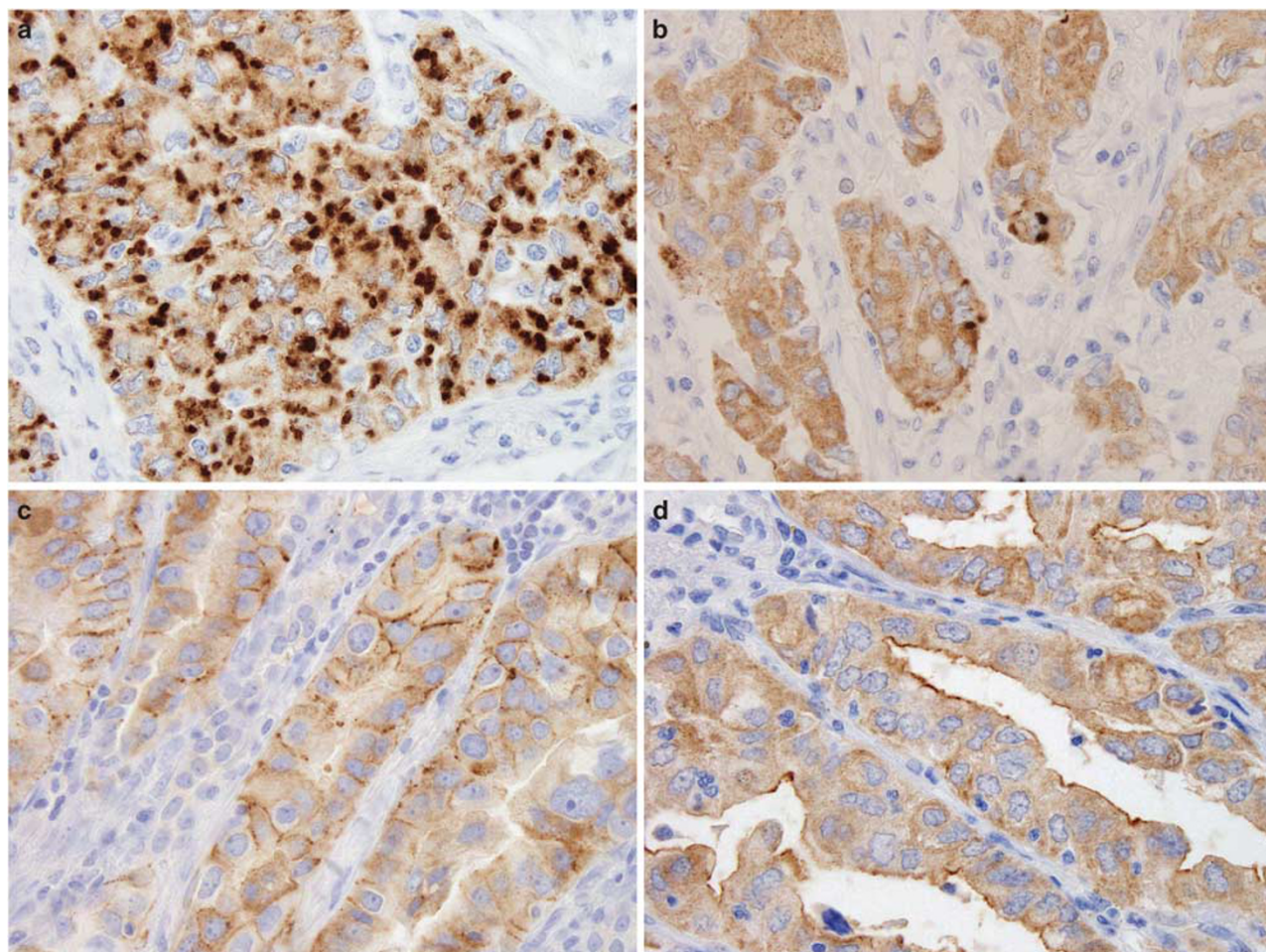


Figure 3 The *ROS1* fusion partner correlated with the *ROS1*-staining pattern. Diffuse (a) or focal (b) intracytoplasmic globular reactivity was observed in 6 of 10 *CD74-ROS1*-positive cancers. Plasma membranous accentuation with a fine granular quality was observed in 3 of 4 *EZR-ROS1*-positive tumors; reactivity localizes to the lateral surface in two cases (c) and along the apical surface in one case (d).

Discussion

We showed here that *ROS1* immunoreactivity significantly differed between *ROS1*-rearranged and -non-rearranged lung adenocarcinoma cohorts. However, unlike the observation by Rimkunas *et al*,⁹ the reactivity in our present study did not separate the cases into two discrete categories that were in perfect concordance with rearrangement status. In contrast, it produced continuous scores that required statistical treatment for practical application. The reason for this discrepancy may be attributed to the technical differences and the difference in the size of the cases. Our finding of *ROS1* expression in 31% of *ROS1*-non-rearranged tumors agrees with those of others. For example, in microarray analyses, *ROS1* mRNA level was significantly elevated in 20–30% of non-small cell lung cancers,¹⁶ and one study¹⁵ specifically documented the *ROS1* mRNA expression independent of gene rearrangement. Similarly, immunohistochemical analyses by Lee *et al*¹⁷ found that 22% of non-small cell lung carcinomas expressed *ROS1*.

Taken together, these data highlight the importance of establishing the optimal immunostaining interpretative criteria to predict gene rearrangement.

In our search for such criteria, we found that an H-score of 150 was a reasonable cutoff because of its 94% sensitivity and 98% specificity. However, H-score-based criteria may not be practical because H-scores are not routinely used in diagnosis. We therefore tested more conventional sets of criteria that are readily applicable to practice and achieved an optimal test performance (94% sensitivity and 90% specificity) by using diffuse ($\geq 75\%$) staining of any intensity to define a positive result. Although we noted similar performance using $\geq 2+$ staining intensity, intensity is relatively subjective and is likely more dependent on the staining protocol. In this regard, a previous study⁹ showed 1+ staining intensity in one-third of the *ROS1*-rearranged tumors tested, although it did not document the extent of reactivity.⁹ The use of diffuse staining as a criterion to indicate gene rearrangement is reasonable because *ROS1* rearrangement is diffusely present within a tumor,⁸ as is typical of early driver

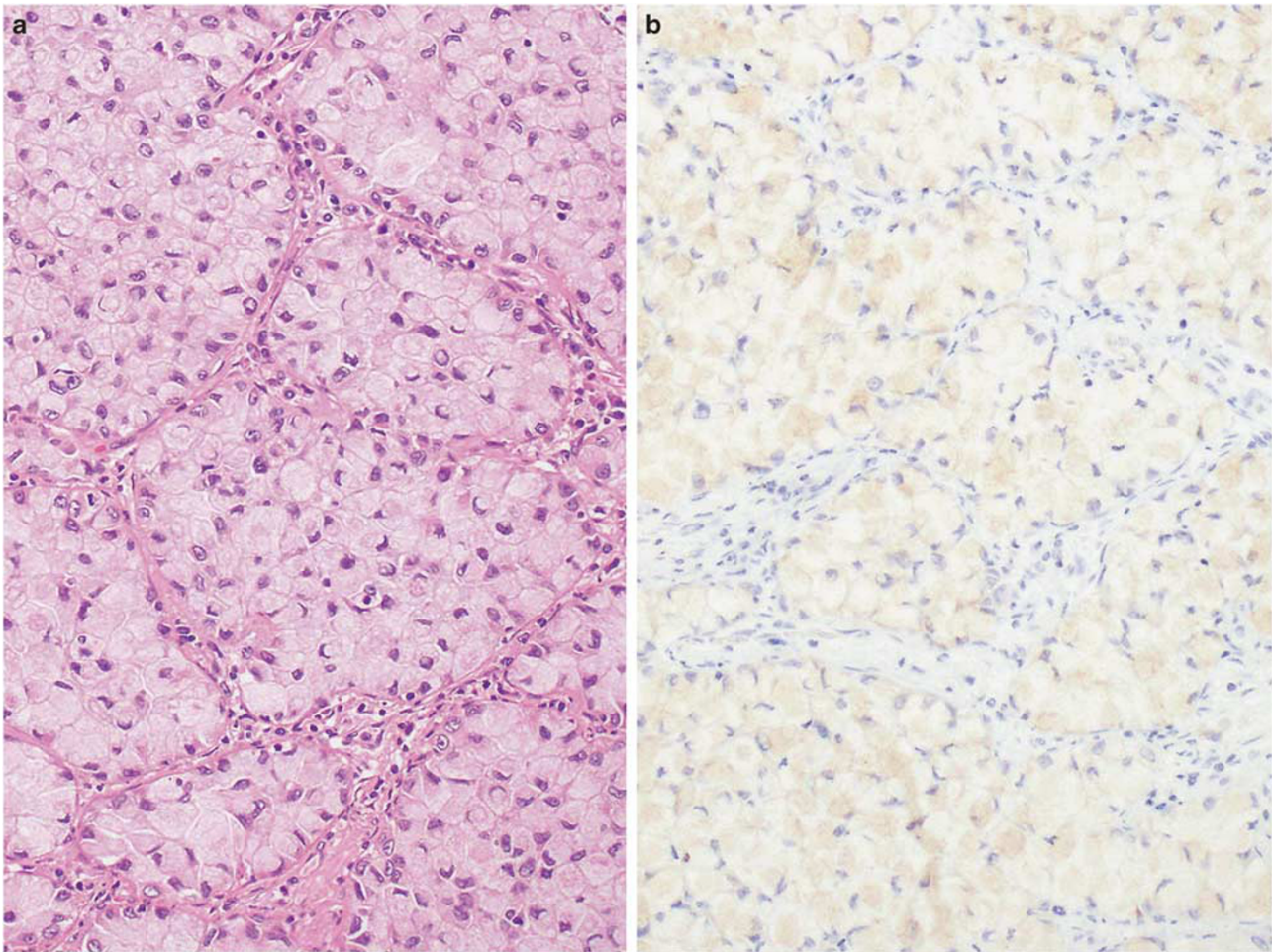


Figure 4 One *EZR-ROS1*-positive signet-ring cell carcinoma (a) showed diffuse but only weak–moderate ROS1 immunoreactivity (b).

genetic changes such as *ALK* rearrangement²¹ and *EGFR* mutation.²²

We noted a correlation between *ROS1* fusion partner genes and the staining patterns, and the result requires validation using a larger cohort. *CD74-ROS1* was significantly associated with at least focal globular immunoreactivity. This pattern probably corresponds to the intracytoplasmic puncta that Rimkunas *et al*⁹ documented in two of the four *CD74-ROS1*-positive lung cancers. The mechanism that generates this unusual staining pattern is unknown but may be related to the physiological localization of the CD74 protein that chaperones MHC class II through the intracellular membrane system.²³ Similarly, the plasma membranous accentuation of reactivity associated with *EZR-ROS1* may reflect the subcellular distribution of ezrin protein that links the plasma membrane with the actin cytoskeleton.²⁴ These characteristic ROS1-staining patterns were not observed in the 78 rearrangement-negative ROS1-expressing cancers in our cohort and, thus, they may be viewed as a rearrangement-specific phenomenon that can be useful for screening. However, we

caution that their recognition may not be straightforward because these patterns may be observed only in a fraction of tumor cells (Figure 3b) and because some *ROS1*-non-rearranged tumors may show at least focal granular staining quality that must be distinguished from CD74-associated globular appearance (compare Figures 1e and 3a).

Our detailed histological analysis of immunohistochemically ‘false-positive’ cases revealed that invasive mucinous adenocarcinomas were over-represented (Figure 1f). It is currently unknown whether the reactivity of these tumors represents true full-length ROS1 overexpression or a nonspecific technical artifact perhaps associated with abundant mucin. In any event, histologic appearance should help determine the likelihood of *ROS1* rearrangement because invasive mucinous adenocarcinomas are typically associated with *KRAS* mutation²⁰ that hardly coexists with *ROS1* rearrangement. Only one invasive mucinous adenocarcinoma with *ROS1* rearrangement has been reported to our knowledge.⁵

There were 2 *ROS1*-rearranged tumors that exhibited less staining than the remaining 15 cases. Case P8 was almost purely composed of signet-ring

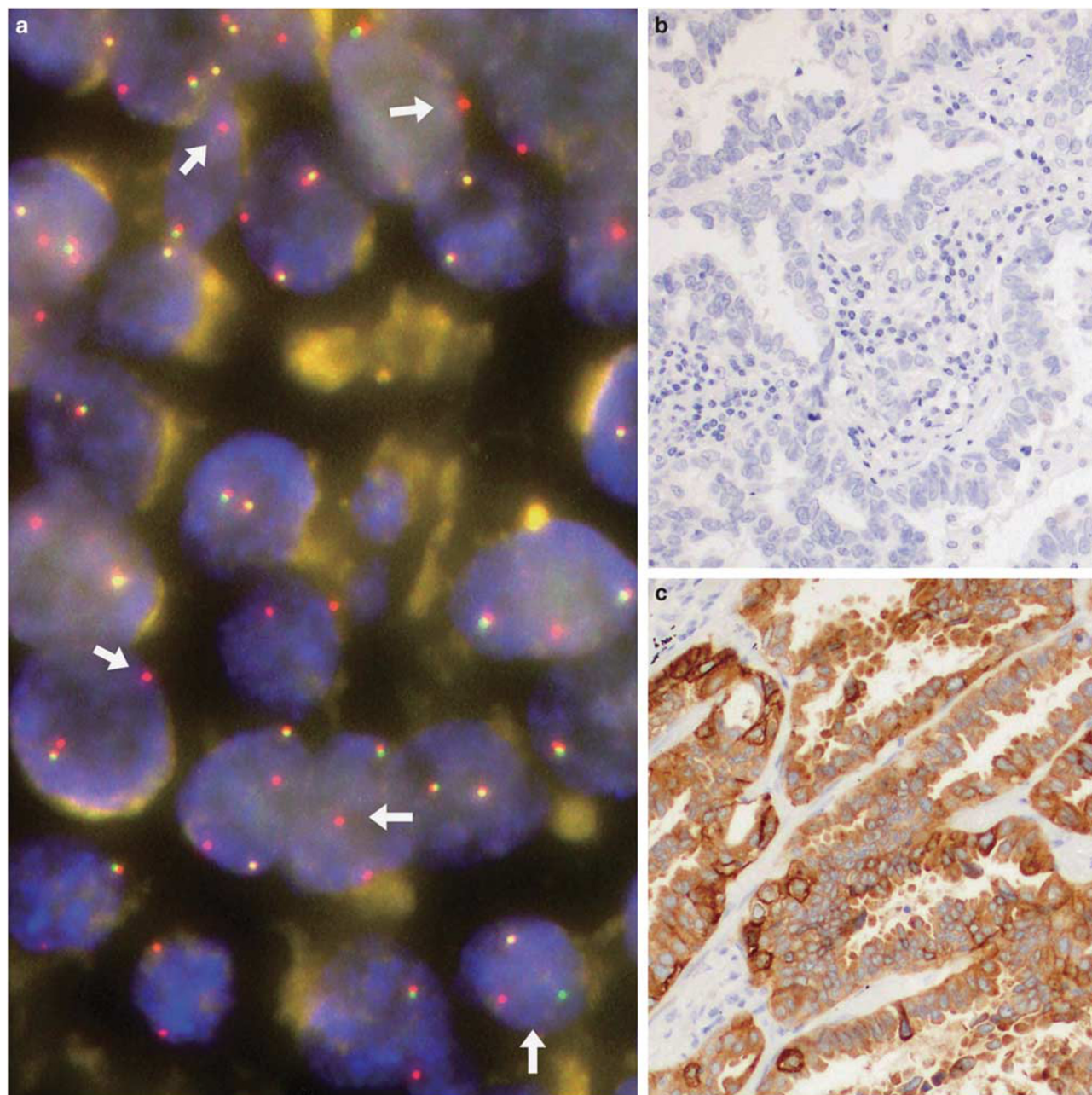


Figure 5 One case showed *ROS1* rearrangement determined using FISH (a, arrows indicate rearranged signals), although no *ROS1* fusion transcript was amplified using multiplex RT-PCR. *ROS1* immunostaining was almost negative (b). The tumor harbored an *EGFR* exon 19 deletion and diffusely expressed mutant *EGFR* as detected using immunohistochemistry (c).

cells and reminds us of a reported pitfall of *ALK* immunohistochemistry for *ALK*-rearranged lung cancers that the staining can be reduced in signet-ring cells.²⁵ Although further study is needed, the potential decrease in immunoreactivity associated with signet-ring cells warrants recognition, particularly because signet-ring cell morphology is characteristic of *ROS1*-rearranged lung cancer.⁸

The other outlier case (P17) posed a greater challenge to interpret because its driver gene status was not clear. Although FISH analysis indicated gene rearrangement, multiplex RT-PCR did not

amplify a *ROS1*-fusion product. Of note, this was the only case in which a discrepancy occurred between FISH and RT-PCR, of all the cases investigated in the present study as well as in our previous study⁸ on *ROS1*-rearranged lung cancers. Although one may explain this discordance by hypothesizing a fusion partner that is not covered by the present RT-PCR design, the very low *ROS1* immunoreactivity (H-score = 5), unlike all other *ROS1*-rearranged cases, casts doubt on the oncological relevance of *ROS1* rearrangement. The presence of an *EGFR* mutation and diffuse strong overexpression of a

mutant EGFR in this case further suggest that the tumor is predominantly addicted to the EGFR signaling with only a minor, if any, contribution from ROS1 activity. Only rarely does *ROS1* rearrangement coexist with *EGFR* mutations in lung cancers, and two cases with such a genotype have been reported to show immunohistochemical coexpression of ROS1 and mutant EGFR.⁹ The present case is, instead, reminiscent of two ALK-immunonegative adenocarcinomas reported by Sasaki *et al*²⁶ that harbored an *ALK*-rearrangement (confirmed by FISH) and an *EGFR* mutation. Future studies such as those using comprehensive sequencing methods may clarify the underlying mechanism that accounts for these unusual disparities. If this case P17 were excluded from the *ROS1*-rearranged cohort, the sensitivity of ROS1 immunohistochemistry would reach 100% by using the criteria that we have proposed (that is, H-score ≥ 150 , extent $\geq 75\%$, or intensity $\geq 2+$).

In summary, our present results agree with those reported by Rimkunas *et al*⁹ in that ROS1 immunohistochemistry by using a newly developed antibody is useful for screening of lung cancer patients for molecular therapy. However, as full-length ROS1 is expressed in a proportion of *ROS1*-non-rearranged cases, establishment of optimal interpretative criteria is critical to achieve concordance with genetic status. High H-score (≥ 150), diffuse extent, or moderate-to-strong staining intensity provide helpful clues to predict *ROS1* rearrangement. Globular reactivity and plasma membranous accentuation correlate with *CD74* and *EZR* as fusion partners, and these patterns are likely to be fusion-specific. Although ROS1 immunohistochemistry is unlikely to replace confirmatory molecular assays, we expect that it will become an integral part of diagnostic algorithm in thoracic oncology. For example, if ROS1 immunostaining is negative or only focally positive, such a case will be almost certainly negative for *ROS1* rearrangement, thus precluding the need of molecular analysis. In contrast, if a diffuse-positive staining is observed, particularly with a moderate–strong intensity, the possibility of *ROS1* rearrangement is high and the case should be sent for molecular confirmation. We further suspect that ROS1 immunohistochemistry may find additional utility in wider clinical field in the future because *ROS1* rearrangements have also been reported in a growing number of non-pulmonary tumors.^{19,27,28}

Acknowledgments

We thank Sachiko Miura, Chizu Kina, Yuko Adegawa, and Ryosuke Yamaga for their superb technical assistance. This work was supported in part by the Program for Promotion of Fundamental Studies in Health Sciences from the National Institute of Biomedical Innovation (NIBIO), Grants-in-Aid from

the Ministry of Health, Labour and Welfare for the 3rd-term Comprehensive 10-year Strategy for Cancer Control, and the National Cancer Center Research and Development Fund. The National Cancer Center Biobank is supported by the National Cancer Center Research and Development Fund, Japan.

Disclosure/conflict of interest

The authors declare no conflict of interest.

References

- 1 Sawabata N, Asamura H, Goya T, *et al*. Japanese Lung Cancer Registry Study: first prospective enrollment of a large number of surgical and nonsurgical cases in 2002. *J Thorac Oncol* 2010;5:1369–1375.
- 2 Kwak EL, Bang YJ, Camidge DR, *et al*. Anaplastic lymphoma kinase inhibition in non-small-cell lung cancer. *N Engl J Med* 2010;363:1693–1703.
- 3 Lynch TJ, Bell DW, Sordella R, *et al*. Activating mutations in the epidermal growth factor receptor underlying responsiveness of non-small-cell lung cancer to gefitinib. *N Engl J Med* 2004;350:2129–2139.
- 4 Rikova K, Guo A, Zeng Q, *et al*. Global survey of phosphotyrosine signaling identifies oncogenic kinases in lung cancer. *Cell* 2007;131:1190–1203.
- 5 Bergethon K, Shaw AT, Ou SH, *et al*. ROS1 rearrangements define a unique molecular class of lung cancers. *J Clin Oncol* 2012;30:863–870.
- 6 Davies KD, Le AT, Theodoro MF, *et al*. Identifying and targeting ROS1 gene fusions in non-small cell lung cancer. *Clin Cancer Res* 2012;18:4570–4579.
- 7 Takeuchi K, Soda M, Togashi Y, *et al*. RET, ROS1 and ALK fusions in lung cancer. *Nat Med* 2012;18:378–381.
- 8 Yoshida A, Kohno T, Tsuta K, *et al*. ROS1-rearranged lung cancer: a clinicopathologic and molecular study of 15 surgical cases. *Am J Surg Pathol* 2013;37:554–562.
- 9 Rimkunas VM, Crosby K, Kelly M, *et al*. Analysis of receptor tyrosine kinase ROS1 positive tumors in non-small cell lung cancer: identification of a FIG-ROS1 fusion. *Clin Cancer Res* 2012;18:4449–4457.
- 10 Suehara Y, Arcila M, Wang L, *et al*. Identification of KIF5B-RET and GOPC-ROS1 fusions in lung adenocarcinomas through a comprehensive mRNA-based screen for tyrosine kinase fusions. *Clin Cancer Res* 2012;18:6599–6608.
- 11 Govindan R, Ding L, Griffith M, *et al*. Genomic landscape of non-small cell lung cancer in smokers and never-smokers. *Cell* 2012;150:1121–1134.
- 12 Seo JS, Ju YS, Lee WC, *et al*. The transcriptional landscape and mutational profile of lung adenocarcinoma. *Genome Res* 2012;22:2109–2119.
- 13 Arai Y, Totoki Y, Takahashi H, *et al*. Mouse model for ROS1-rearranged lung cancer. *PLoS One* 2013;8:e56010.
- 14 Shaw A, Camidge D, Engelman J, *et al*. Clinical activity of crizotinib in advanced non-small cell lung cancer (NSCLC) harboring ROS1 gene rearrangement. *J Clin Oncol* 2012;30:Suppl; abstr 7508.
- 15 Li C, Fang R, Sun Y, *et al*. Spectrum of oncogenic driver mutations in lung adenocarcinomas from East Asian never smokers. *PLoS One* 2011;6:e28204.

- 16 Acquaviva J, Wong R, Charest A. The multifaceted roles of the receptor tyrosine kinase ROS in development and cancer. *Biochim Biophys Acta* 2009;1795:37–52.
- 17 Lee HJ, Seol HS, Kim JY, *et al*. ROS1 receptor tyrosine kinase, a druggable target, is frequently overexpressed in non-small cell lung carcinomas via genetic and epigenetic mechanisms. *Ann Surg Oncol* 2013;20:200–208.
- 18 Fukui T, Ohe Y, Tsuta K, *et al*. Prospective study of the accuracy of EGFR mutational analysis by high-resolution melting analysis in small samples obtained from patients with non-small cell lung cancer. *Clin Cancer Res* 2008;14:4751–4757.
- 19 Charest A, Lane K, McMahon K, *et al*. Fusion of FIG to the receptor tyrosine kinase ROS in a glioblastoma with an interstitial del(6)(q21q21). *Genes Chromosomes Cancer* 2003;37:58–71.
- 20 Travis WD, Brambilla E, Noguchi M, *et al*. International Association for the Study of Lung Cancer/American Thoracic Society/European Respiratory Society International multidisciplinary classification of lung adenocarcinoma. *J Thorac Oncol* 2011;6:244–285.
- 21 Camidge DR, Kono SA, Flacco A, *et al*. Optimizing the detection of lung cancer patients harboring anaplastic lymphoma kinase (ALK) gene rearrangements potentially suitable for ALK inhibitor treatment. *Clin Cancer Res* 2010;16:5581–5590.
- 22 Yatabe Y, Matsuo K, Mitsudomi T. Heterogeneous distribution of EGFR mutations is extremely rare in lung adenocarcinoma. *J Clin Oncol* 2011;29:2972–2977.
- 23 Stumptner-Cuvelette P, Benaroch P. Multiple roles of the invariant chain in MHC class II function. *Biochim Biophys Acta* 2002;1542:1–13.
- 24 Bruce B, Khanna G, Ren L, *et al*. Expression of the cytoskeleton linker protein ezrin in human cancers. *Clin Exp Metastasis* 2007;24:69–78.
- 25 Murakami Y, Mitsudomi T, Yatabe Y. A screening method for the ALK fusion gene in NSCLC. *Front Oncol* 2012;2:24.
- 26 Sasaki T, Koivunen J, Ogino A, *et al*. A novel ALK secondary mutation and EGFR signaling cause resistance to ALK kinase inhibitors. *Cancer Res* 2011;71:6051–6060.
- 27 Lee J, Lee SE, Kang SY, *et al*. Identification of ROS1 rearrangement in gastric adenocarcinoma. *Cancer* 2013;119:1627–1635.
- 28 Gu TL, Deng X, Huang F, *et al*. Survey of tyrosine kinase signaling reveals ROS kinase fusions in human cholangiocarcinoma. *PLoS One* 2011;6:e15640.